Journal of Alloys and Compounds 509 (2011) 7909–7914

Contents lists available at ScienceDirect

Journal of Alloys and Compounds

journal homepage: www.elsevier.com/locate/jallcom

Grain boundary microstructure in DyF_3-diffusion processed Nd–Fe–B sintered magnets

Fang Xu, Jing Wang, Xianping Dong, Lanting Zhang*, Jiansheng Wu

School of Materials Science and Engineering, Shanghai Jiao Tong University, 800 Dong Chuan Road, Shanghai 200240, PR China

ARTICLE INFO

Article history:
Received 23 February 2011
Received in revised form 6 May 2011
Accepted 9 May 2011
Available online 14 May 2011

Keywords:
Nd–Fe–B sintered magnet
Coercivity
Grain boundary
Diffusion
Microstructure

ABSTRACT

The effect of post-sinter tempering on the DyF_3-diffusion processed Nd–Fe–B was investigated using two kinds of starting magnets. The increase of coercivity after diffusion process using as-sintered magnet was higher than that using two-stage tempered magnet. The grain boundary phase of the tempered magnet became discontinuous upon further annealing at the temperature of diffusion process. This clearly indicates that a continuous grain boundary phase is helpful to the DyF_3-diffusion process. When sufficiently diffused, there is no enrichment of Dy in the grain boundary phase. The excess Nd as a result of Dy substitution in the $Nd_2Fe_{14}B$ matrix phase forms Nd–O phase at grain boundary and on the surface of the magnet. The increase of coercivity can be related to the $(Nd,Dy)_2Fe_{14}B$ grains as well as to the improved decoupling by the grain boundary phase.

1. Introduction

In recent years, new methods are being explored to increase the coercivity of Nd–Fe–B sintered magnets using a small amount of heavy rare-earth elements such as Dy and Tb. The grain boundary diffusion process is one of the effective ways to increase coercivity of the magnet with little sacrifice of remanence [1–3]. Instead of direct alloying, heavy rare-earth elements are introduced into the magnet via solid-state reaction during diffusion process. The reported media containing the heavy rare-earth elements can be in the form of metal elements [4,8,9], oxides [2,10], fluorides [1,2,11] and recently low-melting point eutectic alloys [7,12]. After the diffusion process, the heavy rare-earth elements such as Dy or Tb only distribute at the grain boundary and in the outer region of $Nd_2Fe_{14}B$ grains, so the Dy or Tb quantity required for the coercivity enhancement can be reduced. Microstructure observation has found that the Nd in $Nd_2Fe_{14}B$ matrix phase is partially substitution by Dy/Tb and $(Dy/Tb,Nd)_2Fe_{14}B$ with high anisotropic magnetic field is formed. The lattice structure of $(Dy,Nd)_2Fe_{14}B$ is reported to be the same as that of $Nd_2Fe_{14}B$ [13]. According to Sepehri-Amin et al. [4], there was no enrichment of Dy at the grain boundary phase after Dy diffusion process and the composition of the outer region of the $Nd_2Fe_{14}B$ grains changed to $(Dy,Nd)_2Fe_{14}B$. However, many works have reported enrichment of Dy or Tb in the vicinity of grain boundary. Li et al. [5] showed that the grain interface enriched with Dy and Tb could retard the formation of reversed domains. Dy segregation near the grain boundaries was found after diffusion process by rare-earth fluoride liquid coating [6]. Moreover, it was shown that the same magnitude of coercivity enhancement required less Dy [6]. Recently, Oono [7] indicated that a thin layer with an elevated concentration of Dy formed in the $Nd_2Fe_{14}B$ grain regions adjacent to the grain boundary phases after Dy–Ni–Al diffusion process. Thus the conditions to observe the enrichment of Dy or Tb near the grain boundary region should be further clarified.

Since the grain boundary is supposed to be the diffusion path, the microstructure of grain boundary plays an important role in diffusion process. For Nd–Fe–B sintered magnets, heat treatment is known to be an effective way to tune the magnetic properties by changing the microstructure of grain boundary. Many works have shown that the grain boundary phase is discontinuous in as-sintered magnets while it is continuous in tempered magnets [14,15]. Limited attention has been paid to investigate which type of grain boundary will be desirable to diffusion process up to now. In this study, two starting magnets under different heat treatment conditions were designed to investigate their effect on the diffusion process. Moreover, the morphology and chemistry in the grain boundary region and magnetic properties of the diffusion processed Nd–Fe–B sintered magnets were also investigated.

2. Experimental

Bulk magnets were prepared from commercial jet-milled powders $(Nd_{0.8}Pr_{0.2})_{15.5}Fe_{bal}B_6$ (at.%). The powders were compacted under a magnetic field of 1800 kA/m followed by isostatic pressing at 220 MPa. The green compacts were sintered at 1100 °C for 2 h in vacuum, cooled by gas quenching (as-sintered

* Corresponding author. Tel.: +86 21 54747471; fax: +86 21 5474 5197.
E-mail address: lantingzh@sjtu.edu.cn (L. Zhang).

0925-8388/$ – see front matter.
doi:10.1016/j.jallcom.2011.05.023

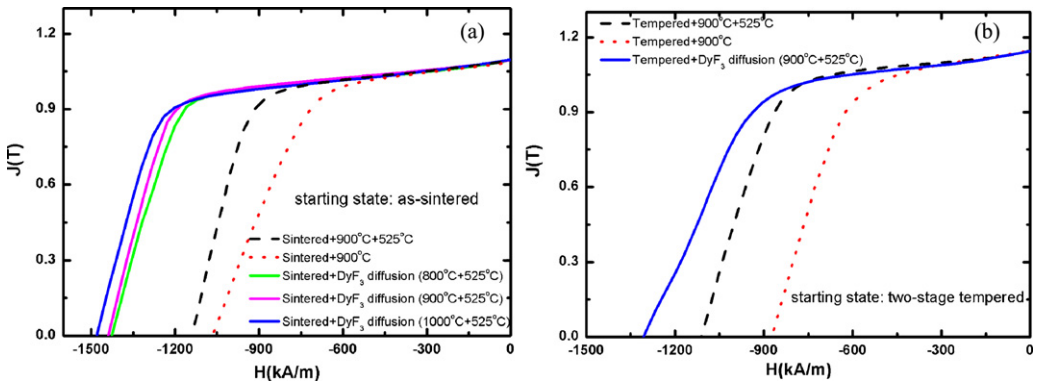

Fig. 1. Demagnetization curves of the Nd–Fe–B magnets without and with diffusion process using (a) the as-sintered and (b) two-stage tempered magnets as the starting material, respectively, measured at 298 K.

state). Some of the as-sintered magnets were further tempered at 900 and 500–560 °C, respectively (tempered state). Both the as-sintered and tempered Nd–Fe–B magnets were used for diffusion process for comparison.

The magnets were cut into small pieces of 2 mm × 3 mm × 3 mm where the preferred magnetization direction was parallel to the 2 mm long edge. DyF_3 powders having a mean particle size of 5 μm were dispersed in ethanol at a proportion of 50 wt% in an ultra-sonic vibrator. Then the small pieces of magnets were immersed in the dispersion for 1 min. After a thin film of DyF_3 was formed on the surfaces of the magnets, the magnets were removed from the dispersion and immediately dried with hot air. The coated magnets were annealed at temperatures between 800 and 1000 °C for 3 h in vacuum and then tempered at 525 °C for 1 h ((sintered or tempered) + DyF_3 diffusion (800–1000 °C + 525 °C)). To monitor the change during diffusion process, magnets without a DyF_3 coating ((sintered or tempered) + 900 °C + 525 °C) were used as a comparison. Moreover, the as-sintered and tempered Nd–Fe–B magnets were annealed at 900 °C ((sintered or tempered) + 900 °C) to investigate their microstructure evolution.

The magnetic properties of the samples were measured using a vibrating sample magnetometer (Lake Shore 7410 VSM) after the magnetic alignment of the samples. Backscattered electron (BSE) images were observed by scanning electron microscope (SEM) (Jeol JSM-7600F). Detailed microstructure at grain boundary was investigated by high resolution transmission electron microscopy (HRTEM) and scanning transmission electronic microscopy (STEM) (Jeol JEM-2100F). Both the microscopes were equipped with an energy dispersive X-ray spectrometer (EDS) (Oxford INCA system).

3. Results and discussion

Fig. 1 compares the room temperature demagnetization curves of the magnets with and without diffusion process. In Fig. 1(a), the as-sintered magnets were used for diffusion process. Compared with the magnets without a DyF_3 coating processed under the same condition, coercivity increased from 1125 to around 1450 kA/m after the diffusion process, while the remanence B_r was almost unchanged (Fig. 1(a)). Diffusion process at temperatures between 800 and 1000 °C resulted in a slight difference in coercivity within 50 kA/m (Fig. 1(a)). However, if a tempered magnet was used as the starting piece, coercivity was below 1350 kA/m after the diffusion process (Fig. 1(b)), which is about 100 kA/m smaller than that of the as-sintered magnets under the same condition. In order to understand the effect of post-sinter tempering on the diffusion process, both the as-sintered and tempered magnets were annealed at 900 °C without a DyF_3 coating. After annealing, the coercivity of the as-sintered magnet was about 1050 kA/m (red dotted line in Fig. 1(a)) while that of the tempered magnet decreased to below 900 kA/m (red dotted line in Fig. 1(b)).

Fig. 2 compares the microstructure of as-sintered and tempered magnets upon further annealing at 900 °C, respectively. In the BSE image, the bright contrast corresponds to phases containing more heavy elements, which is the Nd-rich grain boundary phase in the microstructure. Although the grain boundary phase is not clear along some of the grain boundaries, there is a thin continuous grain boundary phase in the as-sintered magnet upon further annealing at 900 °C (Fig. 2(a)). However, the bright grain boundary phase is found to be discontinuous in the form of particles embedded along the grain boundary in the tempered magnet (Fig. 2(b)). This indicates that further annealing at 900 °C after two-stage tempering results in a discontinuous grain boundary phase in the microstructure. The discontinuous grain boundary phase gives rise to a poor decoupling between the matrix grains, which corresponds well with the observed low coercivity in Fig. 1(b). Since the low melting point grain boundary phase is supposed to be a path for the diffusion process, the continuous or discontinuous distribution of the grain boundary phase in magnet shall have a large impact on the effectiveness of the DyF_3 diffusion process.

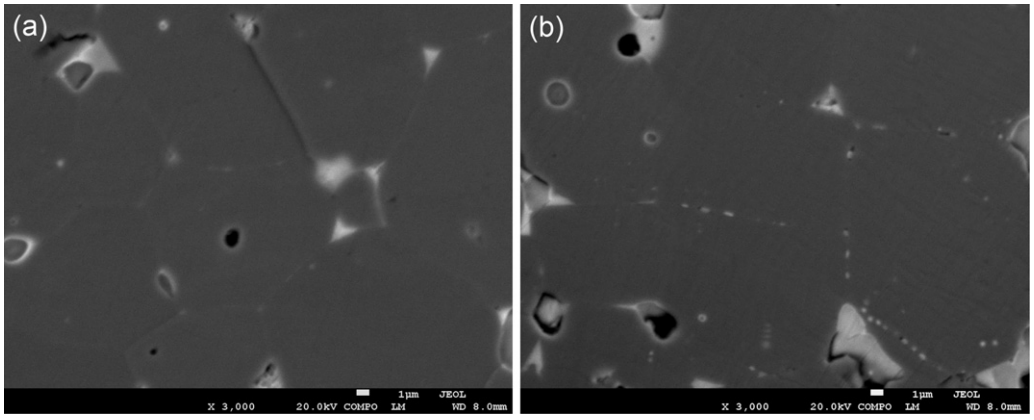

Fig. 2. SEM images of (a) the as-sintered and (b) tempered magnets upon further annealing at 900 °C, respectively.

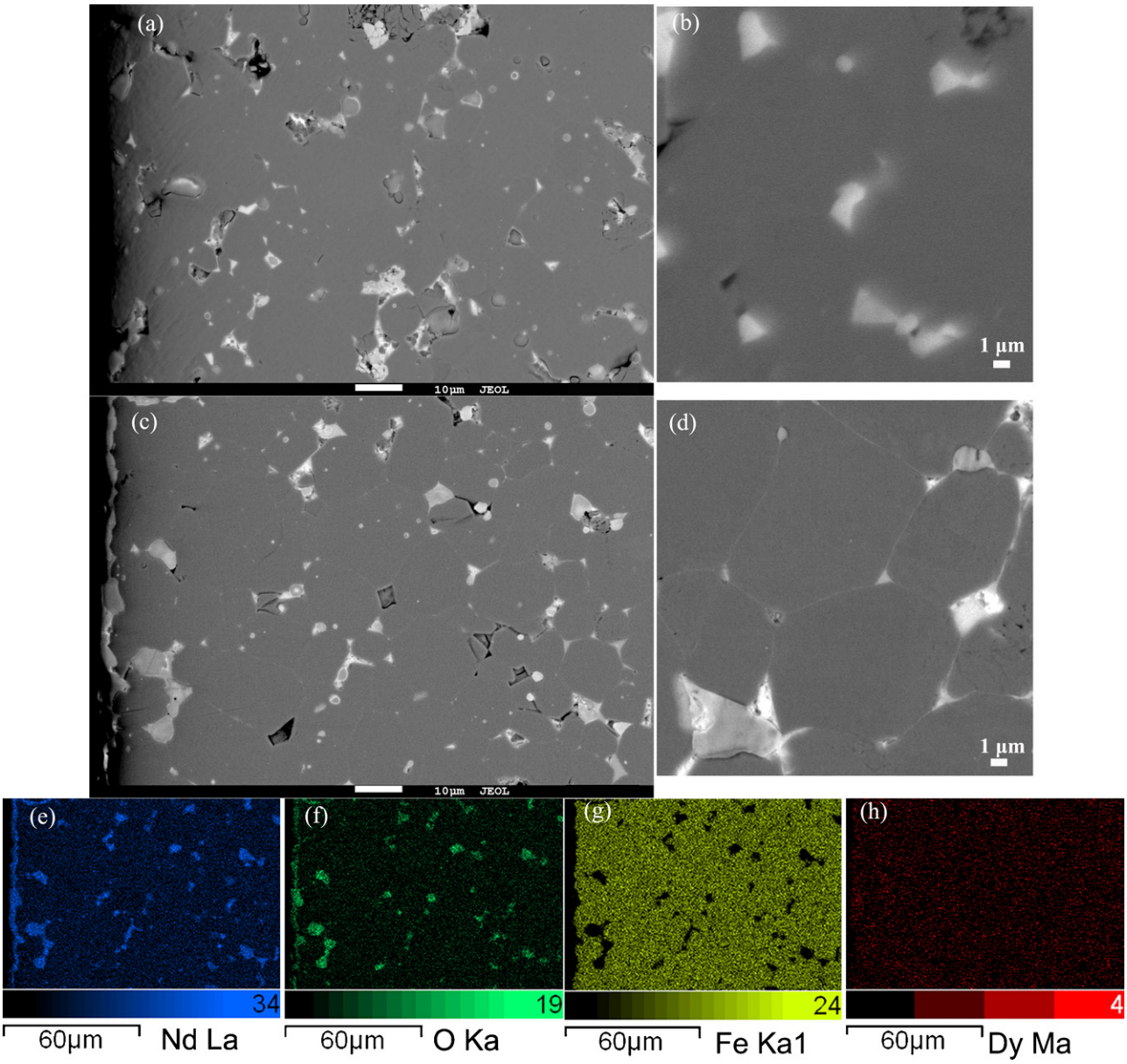

Fig. 3. Cross-sectional SEM images of the magnets without diffusion process (sintered + 900 °C + 525 °C) (a) and (b), and with diffusion process (sintered + DyF_3 diffusion (900 °C + 525 °C)) (c) and (d). (e) Nd Lα, (f) O Kα, (g) Fe Kα1, and (h) Dy Mα are elemental mapping images for (c), respectively.

Cross-sectional SEM images of the magnets with and without DyF_3 diffusion process using the as-sintered magnets as the starting material processed under the same condition are shown in Fig. 3. In Fig. 3(a) and (c), the left-hand side in the images is the outer surface of the magnets. Compared with Fig. 3(a), a ~200 nm thick layer in bright contrast was found on the surface of the magnet after diffusion process (Fig. 3(c)). Element mapping indicated that the layer was rich in Nd and O (Fig. 3(e) and (f)). Since the diffusion process was carried out under vacuum condition, this cover layer is not likely to be the oxidation product but a reaction product after the diffusion process. TEM investigation of the cross section indicated that the cover layer showed an fcc structure whose lattice constant was a_0 = 0.56 nm (Fig. 4). F was detected in this cover layer and the Dy content was slightly higher than that in the matrix phase. Thus the cover layer is probably an Nd-rich phase formed after the diffusion process. Besides the cover layer, the bright grain boundary phase became clear and easily visible in the magnet with diffusion process (Fig. 3(c)). The detailed microstructures of magnets without and with DyF_3 diffusion process using the as-sintered magnets are shown in Fig. 3(b) and (d), respectively. It is shown that the bright grain boundary phase became thick and continuous which is clearly seen in the magnet with DyF_3 diffusion process within the resolution of SEM. However, element mapping did not find obvious enrichment of the Dy element in the microstructure under the present magnification (Fig. 3(h)).

In order to detect the distribution of Dy at different depths, the concentration profiles of Nd, Fe and Dy between the Nd-rich phase and the matrix phase near the surface and 1 mm away from the surface of the magnet after diffusion process using as-sintered and tempered magnets are shown in Fig. 5. Near the surface of the magnets, strong peaks of Dy M_α were found in the cover Nd-rich layer and the outer surface of the $Nd_2Fe_{14}B$ grains (Fig. 5(a) and (d)). However, in the interior region of the magnet (1 mm away from the surface), peaks of Dy were found in the blocky grain boundary phase only (Fig. 5(b) and (e)). No obvious contrast between the periphery and interior of the $Nd_2Fe_{14}B$ grains were found. In contrast, in the diffusion processed magnet using the tempered magnets where the grain boundary phase was discontinuous during the process, there

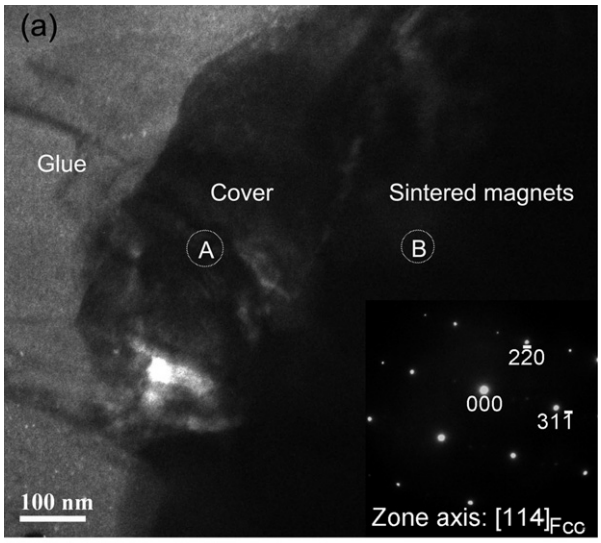

(b) Composition analysis (at. %)

Region	O	F	Nd+Pr	Fe	Dy
A	32.6	10.4	38.4	14.4	4.2
B	/	/	10.3	87.5	2.2

Fig. 4. (a) Cross-sectional TEM image of diffusion processed magnets (sintered + DyF_3 diffusion (900 °C + 525 °C)) and (b) typical compositions determined by EDS (at.%).

is no difference in Dy content between the grain boundary phase and matrix phase under the same depth (Fig. 5(c) and (f)). This is an indication that the Dy diffused into the magnet from the surface through the grain boundary phase, which agrees well with reference [1]. Thus the Dy atoms diffuse into the magnets more easily in the as-sintered magnets where the grain boundary phase is continuous during the process. That should explain why a larger coercivity was obtained in the as-sintered magnet than that in the tempered magnet after the diffusion process.

Fig. 6 shows details of composition distribution in the grain boundary region close to and about 1 mm away from the surface of the diffusion processed magnets using the as-sintered magnet, respectively. The crystalline grain boundary phase lying between the matrix grains was about 10 nm thick. The grain boundary phase in both cases is rich in Nd + Pr and F. There is an obvious enrichment of Dy in the grain boundary phase close to the surface (Figs. 6(a) and (c)). However, in the region about 1 mm away from the surface, Dy was not detected in the thin grain boundary phase, but was detected in the outer shell of the $Nd_2Fe_{14}B$ matrix grain (Figs. 6(b) and (d)). This means that Dy concentration decreases with increasing depth and when sufficiently diffused, the Dy tends to diffuse into the matrix phase from the grain boundary.

In the present investigation, it is found that the effect of the coercivity improvement after the DyF_3 diffusion process depends on the state of the starting magnet. In Nd–Fe–B sintered magnets, many works have shown that the grain boundary phase becomes smooth and continuous upon post-sinter tempering. However, due to the capillary effect, the grain boundary phase in the tempered magnet became discontinuous upon further annealing at 900 °C which

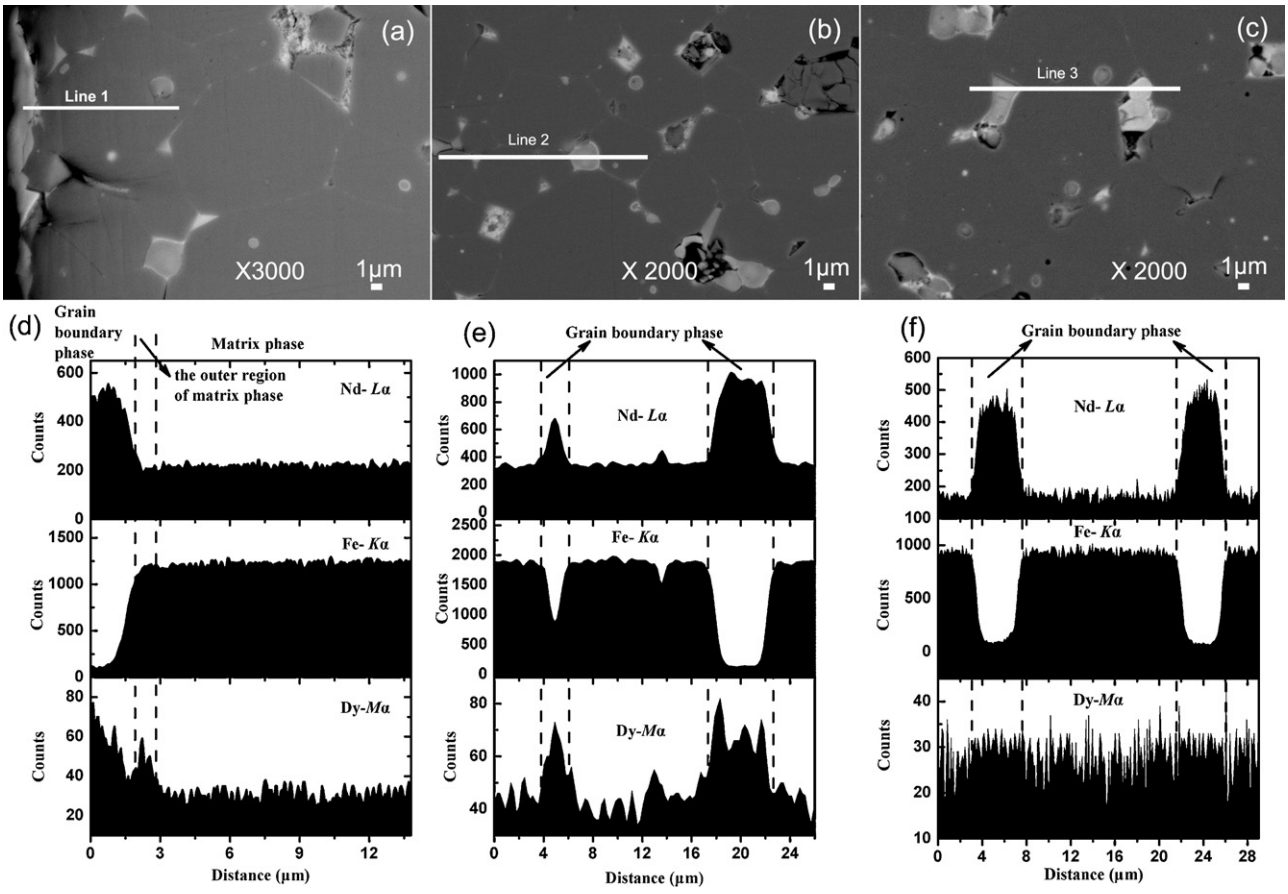

Fig. 5. Cross-sectional SEM images near (a) the surface and (b) 1 mm away from the surface of diffusion processed magnets (sintered + DyF_3 diffusion (900 °C + 525 °C)), (c) the cross-sectional SEM image in the interior region (1 mm away from the surface) of diffusion processed magnet (tempered + DyF_3 diffusion (900 °C + 525 °C)), (d–f) the EDS line profiles taken from line 1, line 2 and line 3 in (a–c), respectively.

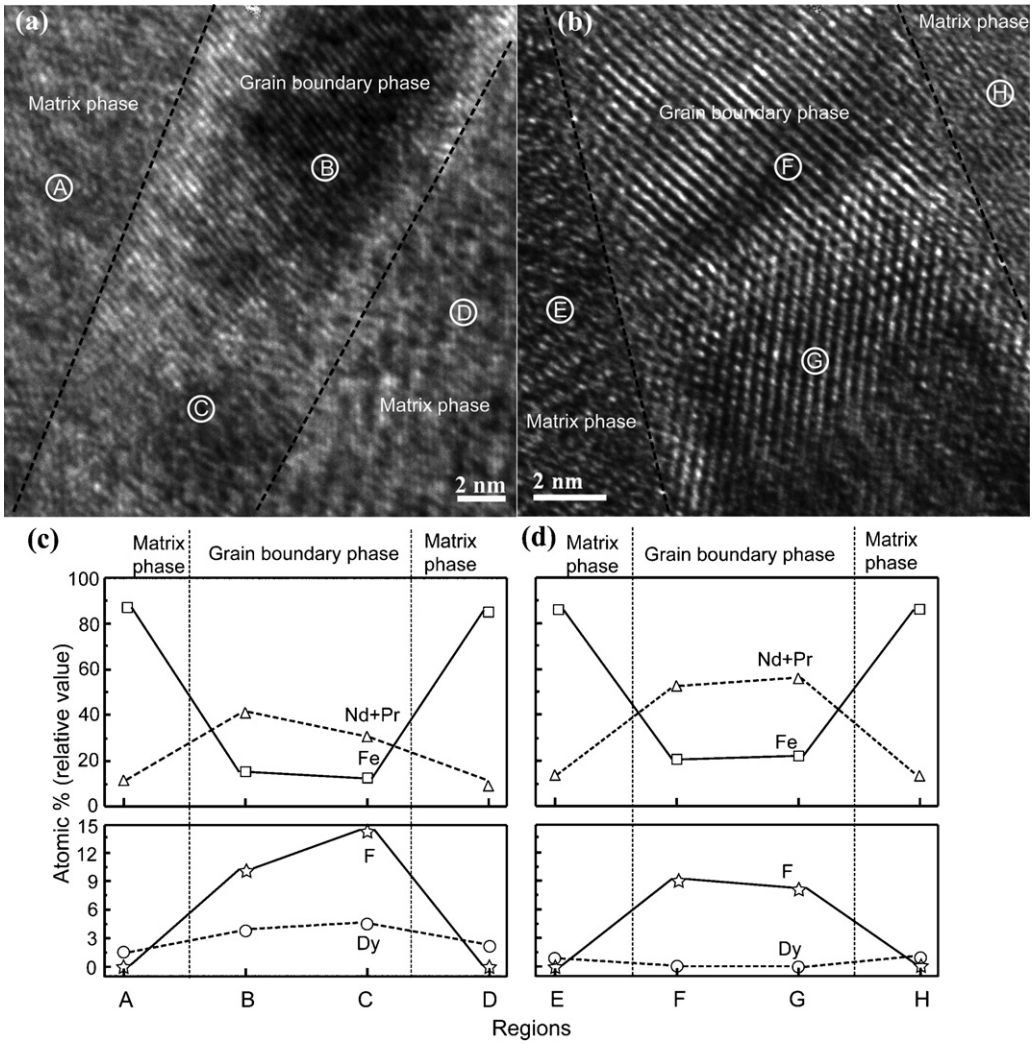

Fig. 6. TEM images of the grain boundary (a) close to the surface and (b) about 1 mm away from surface of diffusion processed magnets (sintered + DyF_3 diffusion (900 °C + 525 °C)), (c) and (d) the element distribution of Nd + Pr, Fe, Dy and F in (a) and (b), respectively.

was the temperature for diffusion process. Thus the diffusion of Dy into the tempered magnet via grain boundary was blocked and the diffusion depth was limited, resulting in a small improvement of coercivity. Besides, fcc-structured Nd–O phase was formed on the surface of the magnet and along the grain boundary in the magnet after the DyF_3 diffusion process. It has been reported that an fcc Nd–O phase instead of dhcp phase on the surface $Nd_2Fe_{14}B$ grains is strongly related to the onset of coercivity in the Nd–Fe–B magnets [16]. Fukagawa et al. [17] has indicated that the formation of an fcc structured NdO_x intergranular phase is essential to the recovery of coercivity in Nd–Fe–B sintered magnets. According to previous investigations [1,2,4–6] and our present observation, Dy favored to substitute for Nd in the $Nd_2Fe_{14}B$ matrix grain to form the $(Nd,Dy)_2Fe_{14}B$ phase. The excess Nd from the matrix grain forms the Nd–O phase at grain boundary and on the surface of the magnet, which is beneficial to the improvement of coercivity due to sufficient decoupling of the matrix grains. In addition, the formation of $(Nd,Dy)_2Fe_{14}B$ in the outer region of the matrix grain adjacent to grain boundary increases the magnetic anisotropy, which is also beneficial to the improvement of coercivity.

4. Conclusions

Two different starting magnets were used for DyF_3 diffusion process to investigate the effect of post-sinter tempering on such a process. The coercivity can be obviously increased after the diffusion process in the as-sintered magnet. The relatively small coercivity increase in the as-tempered magnet under the same process is due to the discontinuous grain boundary phase upon further annealing at 900 °C. This clearly indicates that a continuous grain boundary phase is helpful to the diffusion process. When sufficiently diffused, there is no enrichment of Dy in the grain boundary phase. The excess Nd as a result of Dy substitution in the $Nd_2Fe_{14}B$ matrix phase forms Nd–O phase on the surface of the magnet and at grain boundary in the magnet. The formation of $(Nd,Dy)_2Fe_{14}B$ in the outer region of the matrix grain and the improved decoupling by the grain boundary phase attribute to the coercivity increase.

Acknowledgements

This work is partly supported by the Shanghai-Applied Materials Research & Development Fund (No. 08520740200). TEM observations in this work were performed at Instrumental Analysis Center at Shanghai Jiao Tong University.

References

[1] K. Hirota, H. Nakamura, T. Minowa, M. Honshima, IEEE Trans. Magn. 42 (2006) 2909.
[2] H. Nakamura, K. Hirota, M. Shimao, T. Minowa, M. Honshima, IEEE Trans. Magn. 41 (2005) 3844.

[3] K.T. Park, K. Hiraga, M. Sagawa, Proceedings of the Sixth International Workshop on Rare-Earth Magnets and Their Applications, JIM, Sendai, 2000, p. 257.
[4] H. Sepehri-Amin, T. Ohkubo, K. Hono, J. Appl. Phys. 107 (2010) 09A745.
[5] D. Li, S. Suzuki, T. Kawasaki, K. Machida, Jpn. J. Appl. Phys. 47 (2008) 7876.
[6] M. Komuro, Y. Satsu, H. Suzuki, IEEE Trans. Magn. 46 (2010) 3831.
[7] N. Oono, M. Sagawa, R. Kasada, H. Matsui, A. Kimura, J. Magn. Magn. Mater. 323 (2011) 297.
[8] N. Watanabe, H. Uemoto, M. Ishimaru, M. Itakura, M. Nishida, K. Machida, J. Microsc. 236 (2009) 104.
[9] N. Watanabe, M. Itakura, N. Kuwano, D. Li, S. Suzuki, K. Machida, Mater. Trans. 48 (2007) 915.
[10] X.X. Sun, X.Q. Gao, M.C. Zhang, Q.F. Dong, S.Z. Zhou, J. Chinese Rare Earth Soc. 27 (2009) 86.
[11] H. Suzuki, Y. Satsu, M. Komuro, J. Appl. Phys. 105 (2009) 07A734.
[12] H. Sepehri-Amin, T. Ohkubo, T. Nishiuchi, S. Hirosawa, K. Hono, Scr. Mater. 63 (2010) 1124.
[13] T. Fukagawa, T. Ohkubo, S. Hirosawa, K. Hono, J. Magn. Magn. Mater. 322 (2010) 3346.
[14] Y. shinba, T.J. Konno, K. Ishikawa, K. Hiraga, M. Sagawa, J. Appl. Phys. 97 (2005) 053504.
[15] F. Vial, F. Joly, E. Nevalainen, M. Sagawa, K. Hiraga, K.T. Park, J. Magn. Magn. Mater. 242–245 (2002) 1329.
[16] T. Fukagawa, S. Hirosawa, Scr. Mater. 59 (2008) 183.
[17] T. Fukagawa, S. Hirosawa, T. Ohkubo, K. Hono, J. Appl. Phys. 105 (2009) 07A724.